

Spectral fringes in non-phase-matched SHG and refinement of dispersion relations in the VUV

Peter Trabs,¹ Frank Noack,¹ Aleksandr S. Aleksandrovsky,²
Alexandre I. Zaitsev,² Nikita V. Radionov,² and Valentin Petrov^{1,*}

¹Max Born Institute for Nonlinear Optics and Ultrafast Spectroscopy, 2A Max-Born-Str., Berlin, D-12489, Germany

²L. V. Kirensky Institute of Physics, Akademgorodok 50/38, Krasnoyarsk, 660036, Russia and Siberian Federal University, Svobodny Pr. 79, Krasnoyarsk, 660041, Russia

*petrov@mbi-berlin.de

Abstract: We consider second harmonic generation (SHG) of ultrashort pulses in the case of strong phase- and group-velocity mismatch. Spectral fringes appear in the second harmonic related to two delayed replicas of the fundamental pulse in the time domain. The fringe separation can be used to evaluate the group-velocity and refractive index of nonlinear crystals at extreme wavelengths. Experimental results with femtosecond pulses in SrB₄O₇ (SBO) are used to refine the Sellmeier equation describing the n_c refractive index down to 160 nm, essential for the use of this unique nonlinear crystal for random quasi-phase-matching in the VUV.

©2015 Optical Society of America

OCIS codes: (190.2620) Harmonic generation and mixing; (190.7110) Ultrafast nonlinear optics; (190.4400) Nonlinear optics, materials.

References and links

1. V. Petrov, F. Noack, D. Shen, F. Pan, G. Shen, X. Wang, R. Komatsu, and V. Alex, "Application of the nonlinear crystal SrB₄O₇ for ultrafast diagnostics converting to wavelengths as short as 125 nm," *Opt. Lett.* **29**(4), 373–375 (2004).
2. Yu. S. Oseledchik, A. L. Prosvirnin, A. I. Pisarevskiy, V. V. Starshenko, V. V. Osadchuk, S. P. Belokry, N. V. Svitanko, A. S. Korol, S. A. Krikunov, and A. F. Selevich, "New nonlinear optical crystals: strontium and lead tetraborates," *Opt. Mater.* **4**(6), 669–674 (1995).
3. F. Pan, G. Shen, R. Wang, X. Wang, and D. Shen, "Growth, characterization and nonlinear optical properties of SrB₄O₇," *J. Cryst. Growth* **241**(1-2), 108–114 (2002).
4. A. S. Aleksandrovsky, A. M. Vyunishev, A. I. Zaitsev, A. V. Zamkov, and V. G. Arkhipkin, "Detection of randomized nonlinear photonic crystal structure in a non-ferroelectric crystal," *J. Opt. A, Pure Appl. Opt.* **9**(9), S334–S338 (2007).
5. A. I. Zaitsev, A. S. Aleksandrovsky, A. D. Vasiliev, and A. V. Zamkov, "Domain structure in strontium tetraborate single crystal," *J. Cryst. Growth* **310**(1), 1–4 (2008).
6. M. Baudrier-Raybaut, R. Haïdar, P. Kupecek, P. Lemasson, and E. Rosencher, "Random quasi-phase-matching in bulk polycrystalline isotropic nonlinear materials," *Nature* **432**(7015), 374–376 (2004).
7. P. Trabs, F. Noack, A. S. Aleksandrovsky, A. M. Vyunishev, A. I. Zaitsev, N. V. Radionov, and V. Petrov, "Generation of fs-pulses down to 121 nm by frequency doubling using random quasi-phase-matching in strontium tetraborate," in *Conference Proceedings of Ultrafast Optics IX, Davos, Switzerland, March 4–8, Conference Program, paper Fr2.4*.
8. J.-C. Diels and W. Rudolph, *Ultrashort Laser Pulse Phenomena*, Academic press, Elsevier, 2nd edition, 2006.
9. M. Mlejnek, E. M. Wright, J. V. Moloney, and N. Bloembergen, "Second harmonic generation of femtosecond pulses at the boundary of a nonlinear dielectric," *Phys. Rev. Lett.* **83**(15), 2934–2937 (1999).
10. J. T. Manassah, "Effects of velocity dispersion on a generated second harmonic signal," *Appl. Opt.* **27**(21), 4365–4367 (1988).
11. K. Kato, "Second-harmonic generation to 2048 Å in β-BaB₂O₄," *IEEE J. Quantum Electron.* **22**(7), 1013–1014 (1986).

1. Introduction

Sellmeier equations describing the dispersion of the principal refractive indices of nonlinear optical crystals are normally created from direct measurements of the refractive indices but subsequently refined using phase-matched second-order nonlinear processes, most often

second-harmonic generation (SHG). The situation is, however, complicated in extreme spectral regions and when phase-matching is impossible. Strontium tetraborate, SrB₄O₇ (SBO), is such an example. The birefringence of SBO is too low (<0.005) for phase-matching. Non-phase-matched SHG for temporal diagnostics (autocorrelation measurements) was realized in SBO but the efficiency of this process for a single coherence length was extremely low [1]. On the other hand, the band-gap wavelength (values from absorption measurements differ but indicate in the best case <120 nm [1–3]), the good damage resistivity and chemical stability, and the exceptionally high (1.5–3.5 pm/V [1,4]) value of the diagonal d_{33} element (with respect to the band-gap value) are features that make SBO a unique nonlinear crystal.

SBO exhibits orthorhombic mm2 symmetry but is non-ferroelectric which prevents its electric field poling for quasi-phase-matching (QPM). It was, however, the first non-ferroelectric crystal for which spontaneous formation of random domains was encountered in the process of Czochralski growth [5]. The domains are in the form of sheets normal to the a -axis and rather homogeneous in the other two directions. The static polarization is parallel to the polar two-fold c -axis and the largest nonzero nonlinear coefficient that can be employed is d_{33} . Thus SBO is very attractive for random QPM or RQPM [6] and in a preliminary experiment with femtosecond SHG we generated wavelengths down to 121 nm [7].

The refractive index of SBO was measured down to 212.9 nm [2]. We develop here a method to evaluate the refractive index in the VUV by non-phase-matched SHG with femtosecond pulses. It is based on the measurement of fringes in the second harmonic (SH) spectrum which occur for ultrashort pulse radiation. The latter ensures in turn sufficient efficiency for detection of the SH radiation in the VUV even in the absence of phase-matching. From such measurements down to 160 nm we refine the Sellmeier equation for the n_c refractive index (relevant to the ee-e process involving d_{33}) important for RQPM.

2. Non-phase-matched SHG of ultrashort pulses

For a plane wave packet with a finite spectral distribution around some central frequency the time dependence of the electric field E can be introduced in the usual manner as a product of a fast oscillating term and a slowly varying envelope: $E(t) = (1/2) [\tilde{E}(t) e^{i\omega_c t} + c.c.]$, where $\tilde{E}(t) = |\tilde{E}(t)| e^{i\varphi(t)}$ denotes the complex amplitude, ω_c is the carrier frequency and the complex conjugate ($c.c.$) ensures that the field is real. The complex spectral amplitude can be obtained as a function of the relative frequency $\Omega = \omega - \omega_c$, where ω denotes the instantaneous frequency, by a Fourier transform:

$$\tilde{E}(\Omega) = \int_{-\infty}^{\infty} \tilde{E}(t) e^{-i\Omega t} dt \quad (1)$$

The temporal intensity is $I(t) = \epsilon_0 n c |\tilde{E}(t)|^2 / 2$ and the spectral intensity is given by $S(\Omega) = \epsilon_0 n c |\tilde{E}(\Omega)|^2 / 4\pi$, where ϵ_0 is the electric permittivity of vacuum, c denotes the speed of light in vacuum and n - the refractive index. Let us consider SHG as a particular case of three-wave interaction when the input waves at the fundamental have equal polarizations. This situation corresponds to type-I interaction in birefringent nonlinear crystals, type-0 interaction in QPM or RQPM materials, and can be realized also in the absence of phase-matching if the corresponding nonlinear (coupling) coefficient is non-zero. In the case of ultrashort pulses the SHG process can be described then by only two equations in the laboratory frame (z, t), where the polarization index is omitted for simplicity [8]:

$$\left(\frac{\partial}{\partial z} + \frac{1}{v_F} \frac{\partial}{\partial t} \right) \tilde{E}_F = -i \frac{\chi^{(2)} \omega_F^2}{2c^2 k_F} \tilde{E}_F^* \tilde{E}_{SH} e^{i\Delta k z} \quad (2)$$

$$\left(\frac{\partial}{\partial z} + \frac{1}{v_{SH}} \frac{\partial}{\partial t}\right) \tilde{E}_{SH} = -i \frac{\chi^{(2)} \omega_{SH}^2}{4c^2 k_{SH}} \tilde{E}_F^2 e^{-i\Delta k z} \quad (3)$$

The fundamental (F) and second-harmonic (SH) pulses travel with the corresponding group velocity v_F or v_{SH} . Higher order dispersion terms (group velocity dispersion, GVD) as well as linear losses are neglected, $\chi^{(2)}$ is the effective second order nonlinear susceptibility and $\Delta k = 2k_F - k_{SH}$ denotes the phase-mismatch where the wave vectors $k = n(\omega)\omega/c$ are defined at the corresponding carrier frequencies ω_F and $\omega_{SH} = 2\omega_F$. Since we will consider non-phase-matched SHG, the depletion of the fundamental in Eq. (2) can be neglected (fixed-field approximation) and this equation yields the well-known stationary solution $\tilde{E}_F(t, z) = \tilde{E}_F(t - z/v_F) = \tilde{E}_F(\eta)$. The latter permits to integrate Eq. (3) with respect to the propagation coordinate z which gives, after transformation to the frequency domain [8,9]:

$$\tilde{E}_{SH}(\Omega, d) = -i \frac{\chi^{(2)} \omega_{SH}^2 d}{4c^2 k_{SH}} \text{sinc}\left[(M\Omega - \Delta k) \frac{d}{2}\right] (\tilde{E}_F * \tilde{E}_F)(\Omega), \quad (4)$$

where d is the sample thickness, $M = 1/v_{SH} - 1/v_F$ is the inverse group-velocity mismatch (GVM), and the asterisk denotes convolution. In non-phase-matched SHG, $|\Delta k| \gg |M\Omega_M|$ is satisfied where Ω_M denotes some maximum extension of the SH spectral distribution. Under this assumption the sinc-function can be substituted by a sine-function leading to:

$$\tilde{E}_{SH}(\Omega, d) = i \frac{\chi^{(2)} \omega_{SH}^2}{2c^2 k_{SH} \Delta k} \sin\left[(M\Omega - \Delta k) \frac{d}{2}\right] (\tilde{E}_F * \tilde{E}_F)(\Omega) \quad (5)$$

For the spectral intensity one obtains from Eq. (5):

$$S_{SH}(\Omega, d) = \left(\frac{\chi^{(2)} \omega_{SH}^2}{2c^2 k_{SH} \Delta k}\right)^2 \sin^2\left[(M\Omega - \Delta k) \frac{d}{2}\right] |(\tilde{E}_F * \tilde{E}_F)(\Omega)|^2 \quad (6)$$

Equation (6) indicates that the SH spectrum is completely modulated exhibiting characteristic fringes. The GVM can be derived from the fringe separation for a known sample thickness d . Let us Fourier transform Eq. (5) back to the time domain:

$$\begin{aligned} \tilde{E}_{SH}(t, d) &= \frac{1}{2\pi} \int_{-\infty}^{\infty} \tilde{E}_{SH}(\Omega, d) e^{i\Omega t} d\Omega = i \frac{\chi^{(2)} \omega_{SH}^2}{4\pi c^2 k_{SH} \Delta k} \int_{-\infty}^{\infty} \sin\left[(M\Omega - \Delta k) \frac{d}{2}\right] [(\tilde{E}_F * \tilde{E}_F)(\Omega)] e^{i\Omega t} d\Omega \\ &= i \frac{\chi^{(2)} \omega_{SH}^2}{4\pi c^2 k_{SH} \Delta k} \int_{-\infty}^{\infty} \sin\left[(M\Omega - \Delta k) \frac{d}{2}\right] e^{i\Omega t} d\Omega * \int_{-\infty}^{\infty} [(\tilde{E}_F * \tilde{E}_F)(\Omega)] e^{i\Omega t} d\Omega \\ &= i \frac{\chi^{(2)} \omega_{SH}^2}{2c^2 k_{SH} \Delta k} \int_{-\infty}^{\infty} \sin\left[(M\Omega - \Delta k) \frac{d}{2}\right] e^{i\Omega t} d\Omega * \tilde{E}_F^2(t) \\ &= \frac{\pi \chi^{(2)} \omega_{SH}^2}{2c^2 k_{SH} \Delta k} \left[e^{-\frac{i\Delta k d}{2}} \delta\left(t + \frac{Md}{2}\right) - e^{\frac{i\Delta k d}{2}} \delta\left(t - \frac{Md}{2}\right) \right] * \tilde{E}_F^2(t) \\ &= \frac{\pi \chi^{(2)} \omega_{SH}^2}{2c^2 k_{SH} \Delta k} \left[e^{-\frac{i\Delta k d}{2}} \tilde{E}_F^2\left(t + \frac{Md}{2}\right) - e^{\frac{i\Delta k d}{2}} \tilde{E}_F^2\left(t - \frac{Md}{2}\right) \right] \end{aligned} \quad (7)$$

Finally, for the SH intensity one arrives at:

$$I_{SH}(t, d) \propto I_F^2\left(t + \frac{Md}{2}\right) + I_F^2\left(t - \frac{Md}{2}\right) - \left[e^{i\Delta k d} \tilde{E}_F^2\left(t - \frac{Md}{2}\right) \tilde{E}_F^{*2}\left(t + \frac{Md}{2}\right) + c.c. \right] \quad (8)$$

or in the frame moving with the fundamental input pulse:

$$I_{SH}(\eta, d) \propto I_F^2(\eta) + I_F^2(\eta - Md) - \left[e^{i\Delta k d} \tilde{E}_F^2(\eta - Md) \tilde{E}_F^{*2}(\eta) + c.c. \right] \quad (9)$$

If we assume that the fundamental pulse is unchirped, then Eq. (9) leads to:

$$I_{SH}(\eta, d) \propto I_F^2(\eta) + I_F^2(\eta - Md) - 2 \cos(\Delta kd) I_F(\eta - Md) I_F(\eta) \quad (10)$$

According to Eq. (10) the SH temporal profile consists of two delayed pulses with intensity proportional to the square of the fundamental pulse intensity and an interference term which produces Maker-Terhune type oscillations at short propagation distances when the two pulses overlap in time [9]. The spectral fringes are due to the existence of the two pulses in the time domain [9,10]. Their occurrence can be explained by the fact that in the absence of both phase- and group-velocity matching back-conversion to the fundamental is hindered in the initial and final part of the nonlinear crystal where the SH escapes. The spectral fringes are a consequence of the ultrashort pulse durations considered and originate from the group velocity terms included in Eqs. (2)-(3). For quasi continuous-wave radiation one can assume vanishing M parameter in Eqs. (5)-(6). Spectral fringes can be still observed by tuning the carrier frequency of the fundamental. This changes the coherence length and by expanding the phase-mismatch Δk up to 1st order terms in Ω it is easy to see that the fringe spacing will be the same as in the case of ultrashort pulses. In this case, one obtains from Eq. (10):

$$I_{SH}(\eta, d) \propto I_F^2(\eta) \sin^2\left(\frac{\pi d}{2L_c}\right) \quad (11)$$

which describes the well-known fluctuation of the SH power with the coherence length $L_c = \pi / |\Delta k|$ for quasi continuous-wave radiation. However, this effect and the Maker-Terhune type oscillations with the associated spectral fringes are useless for evaluation of the refractive index in extreme wavelength ranges such as the VUV where both availability of tunable fundamental source and detection of the SH are problematic.

3. Numerical simulation of non-phase-matched SHG in BBO

We choose as an example the numerical simulation of the non-phase-matched SHG for a specific interaction in β -BaB₂O₄ (BBO) which we also realized experimentally.

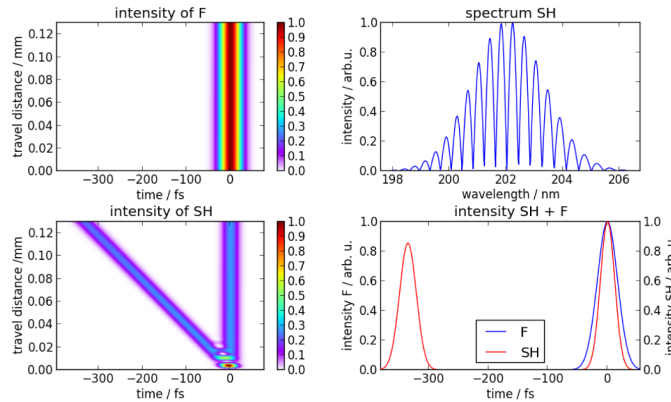


Fig. 1. Non-phase-matched SHG in BBO. Left: Intensity of the fundamental wave and the SH. Right: SH spectrum with fringes, and fundamental and SH pulses at the exit of the crystal.

Pulses of 40 fs duration (FWHM intensity, Gaussian pulse shape assumption) at 404 nm are frequency doubled to 202 nm in a 130 μm thick BBO crystal cut at $\theta = 29^\circ$ for type-I (oo-e) interaction. The polarization of the input fundamental is, however, chosen to be in the critical plane to avoid phase-matching. Due to the fixed azimuthal angle φ , only type-0 (ee-e) interaction exhibits non-zero effective nonlinearity in this case. Equations (2) and (3) are numerically solved by a split-step method where dispersion is taken into account to all orders

in the frequency domain. The Sellmeier equations used for BBO are well established and valid for both wavelengths [11]. Figure 1 illustrates the occurrence of two SH pulses in the time domain in accordance with Eq. (10) as well as the modulation of the SH spectrum. The different intensity/duration of the two pulses (for equal energy) seen is due to the next order (GVD) term not taken into account in the analytical treatment.

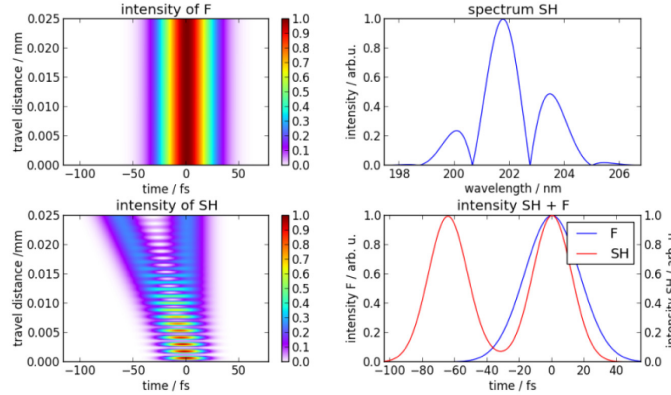


Fig. 2. Same as Fig. 1 but for the initial 25 μm propagation in the BBO crystal.

Figure 2 illustrates the interference pattern in the initial part of the crystal when the two SH pulses overlap in time. While using thin samples relaxes the requirements to the spectral resolution for reliable measurement of the fringes, it can be seen from the figure that the existence of only few fringes will deteriorate the accuracy.

4. Experimental SHG results with SBO and refinement of the Sellmeier equation

Non-phase-matched SHG experiments were performed at fundamental wavelengths of 404 nm (SBO and BBO), 354 nm and 320 nm (SBO only). For input pulse duration of 70 fs, setting Ω_M to one FWHM of the SH spectral amplitude distribution, one arrives at $|\Delta k|/|M\Omega_M| \sim 26$ for BBO which justifies the derivation of Eq. (5). Estimations for SHG at 160 nm in SBO, though based on extrapolations for v_{SH} , yield an even higher ratio of ~ 33 .

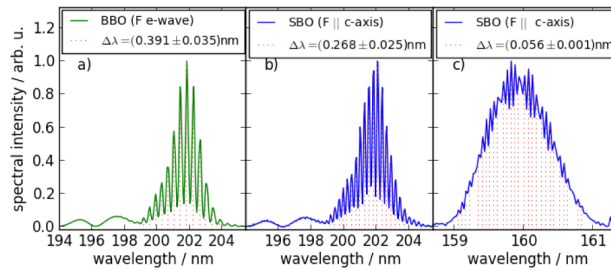


Fig. 3. Measured spectral fringes for non-phase-matched SHG in BBO and SBO.

A 0.423-mm-thick, a -cut SBO crystal was used in this experiment. Note that under the $c < a < b$ convention for the lattice constants [2] the correspondence with the dielectric frame is $abc \equiv yxz$ ($n_x < n_y < n_z$). The SH generated in the ee - e ($\equiv cc$ - c) polarization configuration was measured with a McPherson 0.2 m monochromator Model 234/302 (1200 g/mm grating used in 2nd and 3rd order for better resolution) in combination with a VUV-optimized CCD Camera Andor D0420-BN-995. The slight wedge (1.8 mrad) of the sample made it necessary to reduce the beam diameter to < 2 mm for proper resolution of the fringes. For SHG of 202 nm we employed the frequency doubled output of a femtosecond Ti:sapphire amplifier; for

SHG of 177 and 160 nm the visible output of an optical parametric amplifier (internal SHG of signal) was used after additional external frequency doubling. We tried also to frequency double the 3rd harmonic of the femtosecond Ti:sapphire amplifier at 266 nm but the spectral resolution was insufficient to resolve SH fringes at the 6th harmonic at ~ 133 nm. The experimental accuracy was evaluated by resolving the SH spectra at 202 nm obtained with three different (cut angle and thickness) type-I BBO crystals used in non-phase-matched oo-e and ee-e processes: the experimental fringe separation using the 2nd grating order did not deviate by more than 5% from the calculated value.

Figure 3 shows typical results at 202 nm where a comparison with BBO is possible and at 160 nm. The spectra at 202 nm were recorded in the 2nd grating order. The modulation on the short-wave side in this case is an artifact due to imperfect suppression of the fundamental. The SH spectrum at 160 nm was recorded in the 3rd grating order. The irregular fringe spacing in Fig. 3(c) indicates insufficient sampling of the fringes. Nevertheless the small spacings correspond to 55.7 pm. The SH group velocity in SBO was calculated from the fringe separation $\Delta\Omega$ and the period of the \sin^2 -function in Eq. (6):

$$v_{SH} = (d\Delta\Omega v_F) / (2\pi v_F + d\Delta\Omega) \quad (12)$$

The group velocity at the fundamental was derived from the valid Sellmeier equation [2]. The v_{SH} values at 202, 177, and 160 nm were used as experimental values. They were added to the 9 experimental values available in the literature at longer wavelengths [2].

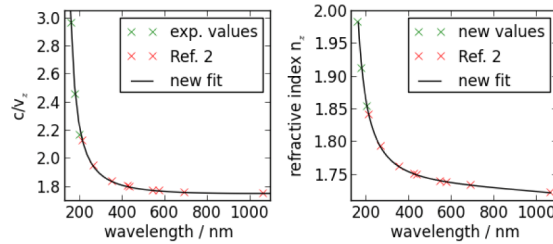


Fig. 4. Experimental data and calculated c/v_z and n_z curves with the refined Sellmeier equation for $n_c \equiv n_z$ of SBO.

An iterative procedure was employed to fit both $c/v_z = n_z - \lambda(\partial n_z / \partial \lambda)$ and n_z , which were analytically expressed from the Sellmeier equation $n_z^2 = A + B/(\lambda^2 - C) - D\lambda^2$ [2]. The initial values used for the parameters A , B , C , and D were those from [2]. The obtained new values for these parameters are: $A = 2.9966$, $B = 0.01271 \mu\text{m}^2$, $C = 0.01203 \mu\text{m}^2$ and $D = 0.03647 \mu\text{m}^{-2}$. Figure 4 shows the experimental data and calculation curves with almost excellent fit. The calculated refractive index at 160 nm is $n_z \approx 1.983$.

5. Conclusion

In the regime of strong phase- and group-velocity mismatch the short pulse SH spectrum is modulated and two SH pulses are formed in the time domain with separation equal to the group delay between the SH and the fundamental. The spectral fringes can be used to estimate the group velocity and fit the refractive index in spectral ranges where direct measurement is difficult, phase-matching is impossible and continuous-wave laser sources are simply not available or will produce too low efficiency to detect the SH. Through such an experiment we refined the Sellmeier equation for the n_c refractive index of SBO, important for RQPM in this material which is transparent in the VUV. The new fit is valid down to 160 nm.